

Constraining disformal couplings with Redshift Space Distortion

Avishek Dusoye¹ , Álvaro de la Cruz-Dombriz^{1,2} , Peter Dunsby¹ and Nelson J. Nunes³

¹Cosmology and Gravity Group, Department of Mathematics and Applied Mathematics, University of Cape Town, Rondebosch 7701, Cape Town, South Africa.

²Universidad de Salamanca, Departamento de Física Fundamental, P. de la Merced, Salamanca, Spain

³Instituto de Astrofísica e Ciências do Espaço, Faculdade de Ciências da Universidade de Lisboa, Campo Grande, PT1749-016 Lisboa, Portugal.

E-mail: avsdus001@myuct.ac.za, alvaro.delacruzdombriz@uct.ac.za, peter.dunsby@uct.ac.za, njnunes@fc.ul.pt

Abstract. We study a quintessence model for which the scalar field is disformally coupled to dark matter. The background mimics the Λ CDM cosmological evolution and the quintessence potential is not specified. A disformal effect due to the quintessential mass is seen in the growth rate of the cosmological structure on large scales. The disformal parameter renders no appreciable effect on the evolution of the total matter perturbation. An analysis of the conformal parameter and quintessential mass is investigated using the Redshift Space Distortion data to find the best-fit values that might explain the well-known σ_8 tension. The best fit of the parameters indicates that the RSD data prefers the model to behave conformally.

Contents

1	Introduction	1
2	Background Cosmology mimicking ΛCDM	2
2.1	Construction of the Dynamical System	4
3	Perturbative Cosmology	5
3.1	The ODEs for the density perturbations of the coupled fluid	6
3.2	The normalised derivative of the interaction term	8
3.3	The normalised derivative of the perturbed interaction	9
4	Results	11
5	Conclusion	15
6	Acknowledgements	16

1 Introduction

In this era of precision cosmology, the parameters of the Λ CDM model have been constrained with great accuracy, due to a wide range of cosmological probes, including Planck's latest results[1–3]. Together with all the compelling evidence for the existence of dark energy [4, 5] and dark matter [6], Λ CDM remains one of the most successful cosmological models from an observational perspective [7, 8]. Nevertheless, the Λ CDM model is unable to explain two phenomena - the unknown nature of the cosmological constant, which is responsible for the accelerated cosmological expansion [9, 10], and the well-known σ_8 tension [11]. This tension arises because the constraints on clustering, which is imposed by the Planck CMB experiment[1], diverges at 2.5σ confidence level from the large-scale measurement by the Dark Energy Surveys (DES)[12, 13]. This tension, therefore, may subtly point to the fact that the Λ CDM model might require some theoretical refinement. Such discrepancy has been a motivation for many attempts to propose several viable theories [14], which could resolve the issue. Extensions of the Λ CDM model can be done by modifying either the cosmological fluids or the Einstein-Hibert action. Preserving the Lovelock theorem [15, 16], such a new action can only be achieved by either considering higher dimensions or non-locality or extra fields [17]. The potential energy of a scalar field can produce the accelerated cosmological expansion, only if it is light enough to change slowly during the Hubble time [18]. The idea of coupled quintessence [18, 19] implies that the scalar field or the quintessence is interacting with another fluid while it evolves with cosmic time. Although the nature of the dark components are not known yet, the possibility of their interaction has not been ruled out [20, 21]. In this article, we firstly assume a quintessence coupled to dark matter and investigate how this coupling influences the evolution of total matter perturbation, as well as the amount of clustering of galaxies. The second assumption deals with the geometry in which this quintessence, ϕ , exists. Let, g_{ab} , be the metric of the gravitational geometry, and \tilde{g}_{ab} as the metric of the physical geometry, then both metrics are related to each other by the disformal transformation [22]:

$$\tilde{g}_{ab} = C(\phi)g_{ab} + D(\phi)\partial_a\phi\partial_b\phi , \quad (1.1)$$

where $C(\phi)$ and $D(\phi)$ are the conformal and disformal functions respectively. In general relativity, $C(\phi) = 1$ and $D(\phi) = 0$. While the effect of the conformal transformation is to rescale the length of original metric g_{ab} [17], the effect of a disformal transformation can be understood as the distortion in angles and lengths of the original metric g_{ab} due to compression, which occurs in the direction of the gradient of the field [22, 23]. The disformal framework has gained attention in the last decade [21, 23–27] and has been applied to many theories such as Horndeski-type scalar tensor theory [28, 29], non-linear massive gravity theory [30, 31] and brane cosmology with higher dimensions [32]. Given this promising avenue to explore, we also assume that the couplings of this coupled quintessence model are of the disformal nature.

One could also construct a coupled quintessence model mimicking the Λ CDM background, so that such a model could both reproduce the successful observational outcome of Λ CDM, and yet have further degrees of freedom to attempt to alleviate the aforementioned anomalies. For instance, a conformally coupled quintessence with a Λ CDM background was investigated [33] in an attempt to alleviate the σ_8 tension. The spherical collapse in coupled quintessence with a Λ CDM background has been reviewed in Ref. [34]. The disformal couplings in Λ CDM background cosmology was studied in Ref. [35].

The novelty in this investigation is the treatment of perturbations for a disformally coupled quintessence model, whose background mimicks Λ CDM. Thus, this article extends the conformally coupled quintessence of [33] toward the disformal framework. This article also builds upon the expansion history of Scenario I investigated in [35]. The effect of quintessential mass and the disformal parameter on the evolution of perturbations is now investigated. Furthermore, an analysis of the disformal parameters, and the quintessential mass are investigated using the Redshift Space Distortion (RSD) data [39–53] to find the best-fit cases of the quintessence model that might explain the well-known σ_8 tension.

The organization of the article is the following. Section 1 provides the motivation of investigating a new perturbation theory for a disformally coupled quintessence model which is mimicking the Λ CDM. Section 2 reviews the background cosmology mimicking Λ CDM. Section 3 treats the derivation of the perturbation evolution equations for a disformally coupled quintessence model, whose background mimics the Λ CDM. Section 4 presents the results and the comparisons with observations.

2 Background Cosmology mimicking Λ CDM

When the Einstein-Hilbert action is extended to the coupled quintessence model, the new action in the Einstein frame is described as:

$$S = \int \left(\frac{1}{2\kappa^2} R + \mathcal{L}_\phi(g_{ab}, \phi) + \mathcal{L}_m(\tilde{g}_{ab}, \psi) \right) \sqrt{-g} \, d^4x, \quad (2.1)$$

with $\mathcal{L}_\phi = -\frac{1}{2}g^{ab}\partial_a\phi\partial_b\phi - V(\phi)$.

The first term is the standard GR gravitational action, with Ricci scalar R and $\kappa^2 \equiv 8\pi G = M_{\text{pl}}^{-2}$. The Planck mass is taken to be $M_{\text{pl}} = 2.4 \times 10^{18}$ GeV with the speed of light and reduced Planck constant set to unity ($\hbar = c = 1$). \mathcal{L}_ϕ is the Lagrangian for the quintessence and consists of a kinetic term and a potential function $V(\phi)$. \mathcal{L}_m is the Lagrangian for matter.

The metric variation of (2.1) with respect to the metric g^{ab} results in the field equations in the Einstein frame.

$$G_{ab} \equiv R_{ab} - \frac{1}{2}g_{ab}R = \kappa^2 T_{ab}^{(tot)} = \kappa^2(T_{ab}^\phi + T_{ab}) , \quad (2.2)$$

where G_{ab} , R_{ab} , T_{ab}^ϕ , and T_{ab} are the Einstein tensor, the Ricci tensor and the energy-momentum tensors for quintessence and matter respectively. The variation of the action (2.1) with respect to the quintessence ϕ results in the modified Klein-Gordon equation [36].

$$\square\phi = V_{,\phi} - Q_0 , \quad (2.3)$$

where $\square \equiv g^{ab}\nabla_a\nabla_b$ is the D'Alembertian operator and $V_{,\phi}$ denotes the derivative of $V(\phi)$ with respect to ϕ . Let "f" denote any general coupled fluid. The conservation equations for the energy-momentum tensors T_{ab}^f and T_{ab}^ϕ in the coupled quintessence model are given below:

$$\nabla^a T_{ab}^\phi = -Q_0 \partial_b \phi , \quad \text{and} \quad \nabla^a T_{ab}^f = +Q_0 \partial_b \phi , \quad (2.4)$$

so that there is a flow of energy and momentum between two coupled fluids in the model, which is governed by the interaction term Q_0 . The total energy-momentum tensor is conserved although their individual components are not separately conserved. For the disformal framework, this interaction term for the coupling between the quintessence and a single fluid can be determined [36].

$$Q_0 = \frac{C_{,\phi}}{2C}T + \frac{D_{,\phi}}{2C}T^{ab}\nabla_a\phi\nabla_b\phi - \nabla_a\left(\frac{D}{C}T^{ab}\nabla_b\phi\right) , \quad (2.5)$$

where $C_{,\phi}$ and $D_{,\phi}$ are the derivatives of conformal and disformal functions $C(\phi)$ and $D(\phi)$ respectively appearing in the disformal transformation (1.1). The spatially flat Friedmann-Lemaître-Robertson-Walker (FLRW) is chosen to be the background metric, where $a(t)$ is the scale factor, t is the cosmic time and $i, j = 1, 2, 3$ denote the spatial coordinates.

$$ds^2 = g_{ab}dx^a dx^b = -dt^2 + a^2(t) \delta_{ij}dx^i dx^j , \quad (2.6)$$

The Friedmann and Raychaudhuri equation for the coupled quintessence can then be obtained [8], where the dot denotes a derivative with respect to cosmic time:

$$H^2 = \frac{\kappa^2}{3}(\rho_\phi + \rho_f) , \quad \dot{H} = -\frac{1}{2}\kappa^2 [(\rho_\phi + P_\phi) + \rho_f(1 + w_f)] , \quad (2.7)$$

where $H \equiv \dot{a}/a$ is the Hubble parameter. Here ρ_f and w_f are the energy density and the equation of state respectively for a general fluid coupled to the quintessence. The energy density and the pressure for the quintessence is denoted by ρ_ϕ and P_ϕ and are defined as:

$$\rho_\phi \equiv \frac{1}{2}\dot{\phi}^2 + V(\phi) \quad \text{and} \quad P_\phi \equiv \frac{1}{2}\dot{\phi}^2 - V(\phi) . \quad (2.8)$$

Assuming a Λ CDM background, ρ_c and ρ_Λ denote the energy density of the cold dark matter and the dark energy in the form of a cosmological constant respectively. When the quintessence is coupled to cold dark matter i.e, $\rho_f = \rho_c$, one can deduce the following:[33, 35].

$$H^2 = \frac{\kappa^2}{3}(\rho_\phi + \rho_f) = \frac{\kappa^2}{3}(\rho_\Lambda + \rho_c) = H_{\Lambda\text{CDM}}^2 \Rightarrow \rho_\phi = \rho_\Lambda , \quad (2.9)$$

$$\dot{H} = -\frac{1}{2}\kappa^2 [(\rho_\phi + P_\phi) + \rho_f(1 + w_f)] = -\frac{1}{2}\kappa^2 [(\rho_\Lambda + P_\Lambda) + \rho_c] = \dot{H}_{\Lambda\text{CDM}} \Rightarrow P_\phi = -\rho_\Lambda , \quad (2.10)$$

$$\Rightarrow V(\phi) = \frac{1}{2}\dot{\phi}^2 + \rho_\Lambda \quad \text{and} \quad V_{,\phi} = \ddot{\phi} . \quad (2.11)$$

Since $V(\phi)$ can be expressed in terms of ϕ and ρ_Λ via Equation (2.11) one does not have to specify the scalar potential. By projecting the conservation equations (2.4) along the velocity of a co-moving observer u_a , we obtain the continuity equations for each fluid:

$$\ddot{\phi} + 3H\dot{\phi} + V_{,\phi} = +Q_0 , \quad (2.12)$$

$$\dot{\rho}_c + 3H\rho_c = -Q_0\dot{\phi} . \quad (2.13)$$

2.1 Construction of the Dynamical System

The dynamical system of this cosmological model can be constructed by defining appropriate dimensionless dynamical variables [36]. The dynamical variable σ measures the strength of the disformal coupling.

$$\begin{aligned} x^2 &\equiv \frac{\kappa^2 \dot{\phi}^2}{3H^2}, & y^2 &\equiv \frac{\kappa^2 \rho_\Lambda}{3H^2}, & z^2 &\equiv \frac{\kappa^2 \rho_c}{3H^2}, & \sigma &\equiv \frac{D(\phi)}{\kappa^2 C(\phi)} H^2, \\ \lambda_C &\equiv -\frac{C_{,\phi}}{\kappa C}, & \lambda_D &\equiv -\frac{D_{,\phi}}{\kappa D}, & \Lambda_C &\equiv \frac{C_{,\phi\phi}}{\kappa^2 C}, & \Lambda_D &\equiv \frac{D_{,\phi\phi}}{\kappa^2 D} . \end{aligned} \quad (2.14)$$

The variables Λ_C and Λ_D are defined for the cases where λ_C and λ_D might be field dependent (See Equation (2.20) and (3.31)). When the continuity equations (2.12) and (2.13) are expressed in terms of the dynamical variables, one can obtain the set of evolution equations in terms of e-fold $N = \ln a$ [35]:

$$x' = -\frac{H'}{H}x - \frac{3x}{2} + \frac{\sqrt{3}\tilde{Q}_0 z^2}{2} , \quad (2.15)$$

$$z' = -\frac{H'}{H}z - \frac{3z}{2} - \frac{\sqrt{3}\tilde{Q}_0}{2}xz , \quad (2.16)$$

$$\sigma' = \left[\sqrt{3}x(\lambda_C - \lambda_D) - 3(x^2 + z^2) \right] \sigma , \quad (2.17)$$

$$\tilde{Q}_0 \equiv \frac{\kappa Q_0}{3H^2 z^2} = \frac{\lambda_C(1 - 6\sigma x^2) + 3\sigma x(x\lambda_D + \sqrt{3})}{2 - 6\sigma x^2 + 3\sigma z^2} , \quad (2.18)$$

where ' denotes derivative with respect to N . These variables (2.14) are constrained to obey the Friedmann and Raychaudhuri equations (2.7), which now become:

$$1 = x^2 + y^2 + z^2 , \quad \text{and} \quad \hat{H} \equiv \frac{H'}{H} = -\frac{3}{2}[x^2 + z^2] \quad \text{and} \quad \frac{H''}{H} = 6(x^2 + z^2) . \quad (2.19)$$

The derivative of the Raychaudhuri equation is also computed and will be useful later in Section 3.3. The derivative of the variables λ_C and λ_D with respect to N are given below:

$$\lambda'_C = \sqrt{3}x(\lambda_C^2 - \Lambda_C) \quad \text{and} \quad \lambda'_D = \sqrt{3}x(\lambda_D^2 - \Lambda_D) . \quad (2.20)$$

Finally, in order to close this system of differential equations, we specify the conformal and disformal coefficients as in the previous literature [36] :

$$C(\phi) = \exp(2\alpha\kappa\phi) , \quad D(\phi) = \frac{\exp(2(\alpha + \beta)\kappa\phi)}{M^4} = D_m^{-4} \exp(2(\alpha + \beta)\kappa\phi) \quad (2.21)$$

$$\lambda_C \equiv -\frac{1}{\kappa} \frac{C_{,\phi}}{C} = -2\alpha , \quad \lambda_D \equiv -\frac{1}{\kappa} \frac{D_{,\phi}}{D} = -2(\alpha + \beta) , \quad (2.22)$$

where the parameters α and β are constants. $M = D_m^{-1}$ is the mass scale in the disformal coupling. For this choice of $C(\phi)$ and $D(\phi)$ which yields λ_C and λ_D as constants, one obtains $\lambda'_C = \lambda'_D = 0$. In a conformal case, the function $D(\phi)$ and its derivatives vanish.

3 Perturbative Cosmology

As mentioned above, the novelty of this investigation is that we shall treat the perturbations of a disformally coupled quintessence model, whose background mimics Λ CDM (See Section 2). We therefore need to study the evolution of the density perturbations for the coupled fluid and the growth factor in this context and compare it to observations.

The scalar perturbations in the Newtonian gauge (i.e., the Bardeen Potential Φ and Ψ) are considered along the FLRW metric, whose line elements are expressed as:

$$ds^2 = -(1 + 2\Phi)dt^2 + a^2(t) \delta_{ij}(1 - 2\Psi)dx^i dx^j. \quad (3.1)$$

Similarly, the energy density ρ_n and the pressure P_n of the n^{th} fluid as well as the scalar field ϕ have been perturbed in order to compute the perturbed energy-momentum tensors:

$$\begin{aligned} \rho_n(\vec{x}, t) &= \bar{\rho}_n(t) + \delta\rho_n(\vec{x}, t), \\ P_n(\vec{x}, t) &= \bar{P}_n(t) + \delta P_n(\vec{x}, t), \\ \phi(\vec{x}, t) &= \bar{\phi}(t) + \chi(\vec{x}, t), \end{aligned} \quad (3.2)$$

so that it will be useful to define the density contrast $\delta_n \equiv \delta\rho_n/\bar{\rho}_n$ and sound speed $c_s^2 \equiv \delta P_n/\delta\rho_n$ of the n^{th} fluid. The scalar modes of the perturbed Einstein equations of (2.2) (i.e. $\delta G_b^a = \kappa^2 \delta T_b^a$) for the coupled quintessence for different combinations of (a, b) are given by the following equations in cosmic time:

$$\nabla^2(\dot{\Psi} + H\Psi) = \frac{\kappa^2 \dot{\phi}}{2} \nabla^2 \chi - \frac{3}{2} aH^2(\Omega_c \theta_c + \Omega_B \theta_B), \quad (3.3)$$

$$a^{-2} \nabla^2 \Psi - 3H(\dot{\Psi} + H\Psi) = \frac{3}{2} H^2(\Omega_c \delta_c + \Omega_B \delta_B) + \frac{\kappa^2}{2} (\dot{\phi} \dot{\chi} - \Psi \dot{\phi}^2 + V_{,\phi} \chi), \quad (3.4)$$

$$\ddot{\Psi} + 4H\dot{\Psi} + (2\dot{H} + 3H^2)\Psi = \frac{3}{2} H^2 c_s^2 (\Omega_c \delta_c + \Omega_B \delta_B) + \frac{\kappa^2}{2} (\dot{\phi} \dot{\chi} - \Psi \dot{\phi}^2 - V_{,\phi} \chi), \quad (3.5)$$

where the equations (3.3)-(3.5) make use of the relation $\Psi = \Phi$, which has been obtained from the traceless spatial components of the perturbed Einstein equations. The variable $\theta_n \equiv \nabla^2 v_n$ is the perturbed co-moving velocity and $\Omega_n = \frac{\kappa \rho_n}{3H^2}$ is the background density parameter for the n^{th} fluid. The subscript “B” denotes baryons. The perturbed Klein-Gordon equation for the quintessence and the perturbed conservation and continuity equations for any general coupled fluid are given below [37].

$$\ddot{\chi} = -3H\dot{\chi} + a^{-2} \nabla^2 \chi - V_{,\phi\phi} \chi + \dot{\phi}(\dot{\Phi} + 3\dot{\Psi}) + \frac{Q_0 \dot{\chi}}{\dot{\phi}} + Q_1 + (2\ddot{\phi} + 6H\dot{\phi})\Phi, \quad (3.6)$$

$$\dot{\delta}_f = -(1 + w_f) \left(\frac{\theta_f}{a} - 3\dot{\Psi} \right) - 3H(c_s^2 - w_f)\delta_f + \frac{Q_0 \dot{\phi}}{\rho_f} \delta_f - \frac{Q_0 \dot{\chi}}{\rho_f} - \frac{Q_1 \dot{\phi}}{\rho_f}, \quad (3.7)$$

$$\dot{\theta}_f = -H(1 - 3w_f)\theta_f - \frac{\dot{w}_f}{1 + w_f} \theta_f - \frac{\nabla^2 \Psi}{a} - \frac{c_s^2 \nabla^2 \delta_f}{(1 + w_f)a} + \frac{w_f \nabla^2 \pi_f}{(1 + w_f)} + \frac{Q_0 \dot{\phi}}{\rho_f} \theta_f + \frac{Q_0 \nabla^2 \chi}{(1 + w_f)\rho_f a}, \quad (3.8)$$

where $V_{,\phi\phi}$ is the second derivative of the potential $V(\phi)$ with respect to quintessence. The equations (3.7) and (3.8) also utilized the relation $\Psi = \Phi$. The variable π_f is the scalar part of the anisotropic shear perturbation π_j^i from the spatial component of the perturbed energy momentum tensor i.e. $T_j^i = (\bar{P} + \delta P)\delta_j^i + \pi_j^i$. The variable π_f is often related to shear stress

σ_f by $\sigma_f = 2\pi_f w_f / 3(1 + w_f)$ in the literature [38]. The term Q_1 is the perturbation of the interaction term Q_0 from (2.5) and is defined in cosmic time as follows [37]:

$$Q_1 = \frac{-\rho_f}{C + D(\rho_f - \dot{\phi}^2)} \left[\mathcal{B}_1 \delta_f + \mathcal{B}_2 \dot{\Phi} + \mathcal{B}_3 \Psi + \mathcal{B}_4 \dot{\chi} + \mathcal{B}_5 \chi \right], \quad (3.9)$$

$$\text{with } \mathcal{B}_1 = \frac{C_{,\phi}}{2}(1 - 3c_s^2) - 3DH\dot{\phi}(1 + c_s^2) - D(V_{,\phi} - Q_0) - D\dot{\phi}^2 \left(\frac{C_{,\phi}}{C} - \frac{D_{,\phi}}{2D} \right), \quad (3.10)$$

$$\mathcal{B}_2 = 3D\dot{\phi}(1 + w_f), \quad (3.11)$$

$$\mathcal{B}_3 = 6DH\dot{\phi}(1 + w_f) + 2D\dot{\phi}^2 \left(\frac{C_{,\phi}}{C} - \frac{D_{,\phi}}{2D} + \frac{Q_0}{\rho_f} \right), \quad (3.12)$$

$$\mathcal{B}_4 = -3DH(1 + w_f) - 2D\dot{\phi} \left(\frac{C_{,\phi}}{C} - \frac{D_{,\phi}}{2D} + \frac{Q_0}{\rho_f} \right), \quad (3.13)$$

$$\begin{aligned} \mathcal{B}_5 = & \frac{C_{,\phi\phi}}{2}(1 - 3w_f) + \frac{(1 + w_f)D\nabla^2}{a^2} - DV_{,\phi\phi} - D_{,\phi}V_{,\phi} - 3D_{,\phi}H\dot{\phi}(1 + w_f) \\ & - D\dot{\phi}^2 \left[\frac{C_{,\phi\phi}}{C} + \left(\frac{C_{,\phi}}{C} \right)^2 + \frac{C_{,\phi}D_{,\phi}}{CD} - \frac{D_{,\phi\phi}}{2D} \right] + \left(C_{,\phi} + D_{,\phi}\rho_f - D_{,\phi}\dot{\phi}^2 \right) \frac{Q_0}{\rho_f}. \end{aligned} \quad (3.14)$$

The ∇^2 operator appearing in the second term of the coefficient \mathcal{B}_5 in (3.14) acts on the variable χ in equation (3.9). The perturbed Einstein equations (3.3)-(3.5), the perturbed conservation and continuity equations (3.6)-(3.8) are used in deriving the second order evolution equations of density perturbations. The corresponding evolution equations for the baryonic density perturbations are however much simpler, because they are not coupled to the quintessence i.e., $Q_0 = Q_1 = 0$ for baryons, and therefore the equations (3.6)-(3.8) take the form below.

$$\dot{\delta}_B = -\frac{\theta_B}{a} + 3\dot{\Psi} \quad \text{and} \quad \dot{\theta}_B = -H\theta_B - \frac{\nabla^2\Psi}{a}. \quad (3.15)$$

The evolution equations of baryonic density perturbations is then obtained, as shown by [33].

$$\delta''_B + \delta'_B \left(2 + \hat{H} \right) - \frac{3}{2} (\Omega_B \delta_B + \Omega_c \delta_c) = 0. \quad (3.16)$$

3.1 The ODEs for the density perturbations of the coupled fluid

The derivation of the second order evolution equations for the density perturbations of the coupled fluid is provided in this subsection. Since in our model, it is cold dark matter which is coupled to quintessence and it is also assumed as a perfect fluid, one can set the variables $w_f = \dot{w}_f = \nabla^2\pi_f = 0$. Moreover in this article, it will be assumed $c_s^2 = 0$, and hence the equations (3.7)-(3.8) simplify to:

$$\dot{\delta}_c = -\frac{\theta_c}{a} + 3\dot{\Psi} + \frac{Q_0\dot{\phi}}{\rho_c}\delta_c - \frac{Q_0\dot{\chi}}{\rho_c} - \frac{Q_1\dot{\phi}}{\rho_c}, \quad (3.17)$$

$$\dot{\theta}_c = - \left(H - \frac{Q_0\dot{\phi}}{\rho_c} \right) \theta_c - \frac{\nabla^2\Psi}{a} + \frac{Q_0\nabla^2\chi}{\rho_c a}. \quad (3.18)$$

By taking the time derivative of equation (3.17) and substituting for $\dot{\theta}_c$ from the equation (3.18), one obtains

$$\ddot{\delta}_c = \left(2H - \frac{Q_0 \dot{\phi}}{\rho_c} \right) \frac{\theta_c}{a} + \frac{\nabla^2 \Psi}{a^2} - \frac{Q_0 \nabla^2 \chi}{\rho_c a^2} + 3\ddot{\Psi} + \frac{Q_0}{\rho_c} \left[\ddot{\phi} \delta_c + \dot{\phi} \dot{\delta}_c - \ddot{\chi} \right. \\ \left. + \left(\frac{\dot{\rho}_c}{\rho_c} \right) \left(\dot{\chi} - \dot{\phi} \delta_c \right) \right] + \frac{\dot{Q}_0}{\rho_c} \left(\dot{\phi} \delta_c - \dot{\chi} \right) - \frac{Q_1}{\rho_c} \left[\ddot{\phi} - \left(\frac{\dot{\rho}_c}{\rho_c} \right) \dot{\phi} \right] - \frac{\dot{Q}_1 \dot{\phi}}{\rho_c}. \quad (3.19)$$

Equation (3.17) can be re-inserted in equation (3.19) to substitute for θ_c/a and the perturbed Einstein equation (3.5), with $c_s^2 = 0$, can be used to replace $\ddot{\Psi}$:

$$\ddot{\delta}_c + \left(2H - \frac{Q_0 \dot{\phi}}{\rho_c} \right) \left(\dot{\delta}_c - 3\dot{\Psi} - \frac{Q_0 \dot{\phi}}{\rho_c} \delta_c + \frac{Q_0 \dot{\chi}}{\rho_c} + \frac{Q_1 \dot{\phi}}{\rho_c} \right) - \frac{\nabla^2 \Psi}{a^2} + \frac{Q_0 \nabla^2 \chi}{\rho_c a^2} \\ + 12H\dot{\Psi} + 3(2\dot{H} + 3H^2)\Psi - \frac{3\kappa^2}{2}(\dot{\phi}\dot{\chi} - \Psi\dot{\phi}^2 - V_{,\phi}\chi) - \frac{\dot{Q}_0 \dot{\phi}}{\rho_c} \delta_c - \frac{Q_0 \ddot{\phi}}{\rho_c} \delta_c - \frac{Q_0 \dot{\phi}}{\rho_c} \dot{\delta}_c \\ + \left(\frac{\dot{\rho}_c}{\rho_c} \right) \frac{Q_0 \dot{\phi}}{\rho_c} \delta_c + \frac{\dot{Q}_0 \dot{\chi}}{\rho_c} + \frac{Q_0 \ddot{\chi}}{\rho_c} - \left(\frac{\dot{\rho}_c}{\rho_c} \right) \frac{Q_0 \dot{\chi}}{\rho_c} + \frac{Q_1 \ddot{\phi}}{\rho_c} + \frac{\dot{Q}_1 \dot{\phi}}{\rho_c} - \left(\frac{\dot{\rho}_c}{\rho_c} \right) \frac{Q_1 \dot{\phi}}{\rho_c} = 0. \quad (3.20)$$

The wave number k appears when performing a Fourier transformation of ∇^2 operator ($\nabla^2 \rightarrow -k^2$). Under the approximation of $k^2 \Psi \gg a^2 H^2 \Psi$ and $k^2 \chi \gg a^2 H^2 \chi$ i.e, the Newtonian limit for sub-Hubble scales, Equation (3.20) reduces into:

$$\ddot{\delta}_c + \left(2H - \frac{Q_0 \dot{\phi}}{\rho_c} \right) \left(\dot{\delta}_c - \frac{Q_0 \dot{\phi}}{\rho_c} \delta_c + \frac{Q_1 \dot{\phi}}{\rho_c} \right) - \frac{\nabla^2 \Psi}{a^2} + \frac{Q_0 \nabla^2 \chi}{\rho_c a^2} - \frac{\dot{Q}_0 \dot{\phi}}{\rho_c} \delta_c \\ - \frac{Q_0 \ddot{\phi}}{\rho_c} \delta_c - \frac{Q_0 \dot{\phi}}{\rho_c} \dot{\delta}_c + \left(\frac{\dot{\rho}_c}{\rho_c} \right) \frac{Q_0 \dot{\phi}}{\rho_c} \delta_c + \frac{Q_1 \ddot{\phi}}{\rho_c} + \frac{\dot{Q}_1 \dot{\phi}}{\rho_c} - \left(\frac{\dot{\rho}_c}{\rho_c} \right) \frac{Q_1 \dot{\phi}}{\rho_c} = 0. \quad (3.21)$$

Similarly, the perturbed Einstein equation (3.4) and the perturbed Klein-Gordon (3.6) can be approximated in the Newtonian limit to render the two following expressions.

$$\frac{\nabla^2 \Psi}{a^2} \approx \frac{3}{2} H^2 (\Omega_c \delta_c + \Omega_B \delta_B) \quad \text{and} \quad \frac{\nabla^2 \chi}{a^2} \approx -Q_1. \quad (3.22)$$

$\nabla^2 \dot{\chi}$ can also be easily computed, which is useful for later derivations in Section 3.3:

$$\frac{\nabla^2 \dot{\chi}}{a^2} \approx -(\dot{Q}_1 + 2HQ_1). \quad (3.23)$$

The expressions in (3.22) are used to substitute $\nabla^2 \Psi$ and $\nabla^2 \chi$, which appear in the evolution equation (3.21). Thus, after substituting (3.22) and $\dot{\rho}_c/\rho_c$ (using equation (2.13)) into (3.21), one obtains

$$\ddot{\delta}_c + 2\dot{\delta}_c \left(H - \frac{Q_0 \dot{\phi}}{\rho_c} \right) - \delta_c \left[5H \left(\frac{Q_0 \dot{\phi}}{\rho_c} \right) + \frac{\dot{Q}_0 \dot{\phi}}{\rho_c} + \frac{\dot{Q}_0 \ddot{\phi}}{\rho_c} \right] + 5H \left(\frac{Q_1 \dot{\phi}}{\rho_c} \right) \\ - \frac{3}{2} H^2 (\Omega_c \delta_c + \Omega_B \delta_B) - \frac{Q_0 Q_1}{\rho_c} + \frac{Q_1 \ddot{\phi}}{\rho_c} + \frac{\dot{Q}_1 \dot{\phi}}{\rho_c} = 0. \quad (3.24)$$

Using the dynamical variables defined in (2.14), all the functions and derivatives of Equation (3.24) can be re-expressed in terms of the time variable N . One can use (2.18) and further define these normalised variables;

$$\tilde{Q}_0 \equiv \frac{\kappa Q_0}{3H^2 z^2}, \quad \tilde{Q}_1 \equiv \frac{\kappa Q_1}{3H^2 z^2}, \quad \hat{q}_0 \equiv \frac{\kappa Q'_0}{3H^2 z^2}, \quad \hat{q}_1 \equiv \frac{\kappa Q'_1}{3H^2 z^2}. \quad (3.25)$$

THis yields the following expression:

$$\begin{aligned} \delta''_c = & -\delta'_c \left(2 - 2\sqrt{3}\tilde{Q}_0 x + \hat{H} \right) + \sqrt{3}\delta_c \left[5\tilde{Q}_0 x + \hat{q}_0 x + \tilde{Q}_0 \left(x' + \hat{H}x \right) \right] - 5\sqrt{3}\tilde{Q}_1 x \\ & + \frac{3}{2}(z^2\delta_c + \Omega_B\delta_B) + 3\tilde{Q}_0\tilde{Q}_1 z^2 - \sqrt{3}\tilde{Q}_1 \left(x' + \hat{H}x \right) - \sqrt{3}\hat{q}_1 x. \end{aligned} \quad (3.26)$$

While the tilde denotes the normalisation of the interaction term Q_0 and of its perturbation Q_1 , the hat denotes the normalisation of the derivative of the interaction term Q'_0 and the derivative of its perturbation Q'_1 . After plugging the conservation equation (2.15) to replace $(x' + \hat{H}x)$ in equation (3.26), the second order evolution equation for the density perturbations of the coupled fluid is computed after some manipulations:

$$\begin{aligned} \delta''_c + \delta'_c \left(2 - 2\sqrt{3}\tilde{Q}_0 x + \hat{H} \right) - \delta_c \left[\sqrt{3}\hat{q}_0 x + \frac{\tilde{Q}_0}{2} \left(7\sqrt{3}x + 3\tilde{Q}_0 z^2 \right) \right] \\ + \sqrt{3}\hat{q}_1 x + \frac{\tilde{Q}_1}{2} \left(7\sqrt{3}x - 3\tilde{Q}_0 z^2 \right) - \frac{3}{2}(z^2\delta_c + \Omega_B\delta_B) = 0, \end{aligned} \quad (3.27)$$

where the derivation of \hat{q}_0 and \hat{q}_1 is provided in the next two Section 3.2 and 3.3. Equation (3.27) reduces to the obtained perturbation equation in [33] in the conformal framework (i.e, $D(\phi) = \sigma = 0$).

3.2 The normalised derivative of the interaction term

The interaction term $Q(\phi)$ for a single coupled fluid can be computed by evaluating the covariant derivative of time components for the energy-momentum tensor in equation (2.5) as below. In this section, the derivation is kept general for arbitrary choices of λ_C and λ_D .

$$Q(\phi) = -\frac{C_{,\phi}}{2C}(1 - 3w_f)\rho_f - \left(\frac{D_{,\phi}}{2D} - \frac{C_{,\phi}}{C} \right) \frac{D\dot{\phi}^2}{C} \rho_f + Q_0 \frac{D\dot{\phi}^2}{C} + 3\frac{D}{C}w_f\rho_f H\dot{\phi} - \frac{D\ddot{\phi}}{C}\rho_f. \quad (3.28)$$

The dynamical variables (2.14) are then plugged into equation (3.28) to obtain the following:

$$\begin{aligned} (1 - 3\sigma x^2) \left(\frac{\kappa Q_0}{3H^2 z^2} \right) = & \frac{\lambda_C}{2}(1 - 3w_f) + 3\sqrt{3}w_f\sigma x - \sqrt{3}\frac{\sigma}{H} \left(\dot{x} + \frac{\dot{H}}{H}x \right) \\ & + \frac{3}{2}(\lambda_D - 2\lambda_C)\sigma x^2. \end{aligned} \quad (3.29)$$

The equation of state for coupled dark matter is obtained by setting $w_f = 0$. When the equation (3.29) is expressed in terms of e-fold N and the conservation equation (2.15) is used to replace $(x' + \hat{H}x)$, one obtains the interaction term (2.18) as expected.

The derivative of the equation (3.29) with respect to cosmic time is carried out and is expressed in terms of e-fold N to yield:

$$\begin{aligned} (1 - 3\sigma x^2) \left(\frac{\kappa Q'_0}{3H^2 z^2} \right) &= 2(1 - 3\sigma x^2) \left(\frac{\kappa Q_0}{3H^2 z^2} \right) \left(\frac{H'}{H} + \frac{z'}{z} \right) + \frac{\kappa Q_0}{H^2 z^2} (\sigma' x^2 + 2\sigma x' x) \\ &+ \frac{\lambda'_C}{2} + \frac{3}{2}(\lambda'_D - 2\lambda'_C)\sigma x^2 + \frac{3}{2}(\lambda_D - 2\lambda_C)(\sigma' x^2 + 2\sigma x x') - \sqrt{3} \left(\sigma' - \frac{H'}{H} \sigma \right) \left(x' + \frac{H'}{H} x \right) \\ &- \sqrt{3}\sigma \left[x'' + 2\frac{H'}{H} x' + \frac{H''}{H} x \right]. \end{aligned} \quad (3.30)$$

The conservation equations (2.15) and (2.16) are used to substitute for $(x' + \hat{H}x)$ and z'/z respectively. The derivative of Raychaudhuri equation in (2.19) is used to replace H''/H . Some of the terms get simplified with the normalised variables (3.25) and together with the choice $\lambda'_C = \lambda'_D = 0$ in equation (2.22). The normalised derivative \hat{q}_0 , which is required in the evolution equation (3.27), is then obtained:

$$\begin{aligned} \hat{q}_0 &= -\tilde{Q}_0 \left(3 + \sqrt{3}\tilde{Q}_0 x \right) + \left(3\tilde{Q}_0 + \frac{3}{2}(\lambda_D - 2\lambda_C) \right) \left(\frac{\sigma' x^2 + 2\sigma x x'}{1 - 3\sigma x^2} \right) \\ &+ \frac{\sqrt{3}}{2} \left(\frac{\sigma' - \hat{H}\sigma}{1 - 3\sigma x^2} \right) \left(3x - \sqrt{3}\tilde{Q}_0 z^2 \right) - \sqrt{3}\sigma \left[\frac{x'' + 2\hat{H}x' + 6x(x^2 + z^2)}{1 - 3\sigma x^2} \right]. \end{aligned} \quad (3.31)$$

3.3 The normalised derivative of the perturbed interaction

The perturbed interaction term Q_1 , which is given by (3.9)-(3.14) is re-expressed in terms of the dynamical variables (2.14) in cosmic time as follows. In this section, the derivation is kept general for arbitrary choices of λ_C and λ_D :

$$\kappa Q_1 = \frac{-3H^2 z^2}{(1 - 3\sigma x^2 + 3\sigma z^2)} \left[\mathcal{A}_1 \delta_f + \mathcal{A}_2 \dot{\Phi} + \mathcal{A}_3 \Psi + \mathcal{A}_4 \dot{\chi} + \mathcal{A}_5 \chi \right], \quad (3.32)$$

$$\text{with } \mathcal{A}_1 = -\frac{\lambda_C}{2} - \frac{\sqrt{3}\sigma}{H} \left(\dot{x} + \frac{\dot{H}}{H} x \right) - \frac{3\sigma x^2}{2} (\lambda_D - 2\lambda_C), \quad (3.33)$$

$$\mathcal{A}_2 = \frac{3\sqrt{3}}{H} (1 + w_f) \sigma x, \quad (3.34)$$

$$\mathcal{A}_3 = 6\sqrt{3}(1 + w_f) \sigma x + 3\sigma x^2 \left(\lambda_D - 2\lambda_C + 2 \frac{\kappa Q_0}{3H^2 z^2} \right), \quad (3.35)$$

$$\mathcal{A}_4 = -3 \frac{\kappa \sigma}{H} (1 + w_f) - \sqrt{3} \frac{\kappa \sigma}{H} x \left(\lambda_D - 2\lambda_C + 2 \frac{\kappa Q_0}{3H^2 z^2} \right), \quad (3.36)$$

$$\begin{aligned} \mathcal{A}_5 &= \frac{\kappa \Lambda_C}{2} - \frac{\kappa \sigma}{a^2 H^2} (1 + w_f) \nabla^2 - \frac{\kappa \sigma}{H^2} V_{,\phi\phi} + \lambda_D \frac{\kappa^2 \sigma}{H^2} V_{,\phi} - 3\sqrt{3} \kappa \sigma \lambda_D x (1 + w_f) \\ &- 3\kappa \sigma x^2 \left(\Lambda_C + \lambda_C^2 + \lambda_C \lambda_D + \frac{\Lambda_D}{2} \right) - \kappa (\lambda_C + 3\lambda_D \sigma (z^2 - x^2)) \frac{\kappa Q_0}{3H^2 z^2}, \end{aligned} \quad (3.37)$$

such that the functions \mathcal{A}_m are re-normalised as $\mathcal{A}_m \equiv \mathcal{B}_m / \kappa C$ with $m = 1, \dots, 5$. The ∇^2 operator appearing in the second term of the coefficient \mathcal{A}_5 in (3.37) is acting upon the variable χ in equation (3.32). The relation $\Psi = \Phi$ was applied to equation (3.32) and the equation of state was set to $w_f = 0$ since the coupled fluid is dark matter in this model.

Under the approximation of the Newtonian limit, the perturbed interaction term (3.32) then reduces to the following:

$$\kappa Q_1 (1 - 3\sigma x^2 + 3\sigma z^2) \approx -3H^2 z^2 [\mathcal{A}_1 \delta_c + \mathcal{A}_5 \chi] \approx -3H^2 z^2 \left[\mathcal{A}_1 \delta_c - \frac{\kappa \sigma}{H^2} \left(\frac{\nabla^2 \chi}{a^2} \right) \right], \quad (3.38)$$

where only the second term of the coefficient \mathcal{A}_5 in equation (3.37) survives because it is of same order of $k^2 \chi$. After substituting $a^{-2} \nabla^2 \chi \approx -Q_1$ i.e, the approximation (3.22) of the perturbed Klein Gordon equation and inserting for the normalised variable \tilde{Q}_1 as defined in equation (3.25), one can simplify to obtain:

$$\tilde{Q}_1 \approx -\frac{\mathcal{A}_1 \delta_c}{(1 - 3\sigma x^2 + 6\sigma z^2)}. \quad (3.39)$$

The derivative of perturbed interaction term (3.32) with respect to cosmic time is:

$$\begin{aligned} \kappa \dot{Q}_1 (1 - 3\sigma x^2 + 3\sigma z^2) - \kappa Q_1 (3\dot{\sigma} x^2 + 6\sigma x \dot{x} - 3\dot{\sigma} z^2 - 6\sigma z \dot{z}) &= -6(H \dot{H} z^2 + \\ &+ H^2 z \dot{z}) [\mathcal{A}_1 \delta_c + \mathcal{A}_2 \dot{\Phi} + \mathcal{A}_3 \Psi + \mathcal{A}_4 \dot{\chi} + \mathcal{A}_5 \chi] - 3H^2 z^2 [\dot{\mathcal{A}}_1 \delta_c + \mathcal{A}_1 \dot{\delta}_c + \dot{\mathcal{A}}_2 \dot{\Phi} + \\ &\mathcal{A}_2 \ddot{\Phi} + \dot{\mathcal{A}}_3 \Psi + \mathcal{A}_3 \dot{\Psi} + \dot{\mathcal{A}}_4 \dot{\chi} + \mathcal{A}_4 \ddot{\chi} + \dot{\mathcal{A}}_5 \chi + \mathcal{A}_5 \dot{\chi}]. \end{aligned} \quad (3.40)$$

After applying the relation $\Psi = \Phi$, equation (3.40) reduces under the Newtonian limit to:

$$\begin{aligned} \kappa \dot{Q}_1 (1 - 3\sigma x^2 + 3\sigma z^2) &= \kappa Q_1 (3\dot{\sigma} x^2 + 6\sigma x \dot{x} - 3\dot{\sigma} z^2 - 6\sigma z \dot{z}) - 6(H \dot{H} z^2 + H^2 z \dot{z}) \mathcal{A}_1 \delta_c \\ &- 6(H \dot{H} z^2 + H^2 z \dot{z}) \mathcal{A}_5 \chi - 3H^2 z^2 [\dot{\mathcal{A}}_1 \delta_c + \mathcal{A}_1 \dot{\delta}_c] - 3H^2 z^2 \dot{\mathcal{A}}_5 \chi - 3H^2 z^2 \mathcal{A}_5 \dot{\chi}, \end{aligned} \quad (3.41)$$

where only the second term of the coefficient \mathcal{A}_5 as per (3.37) and its derivatives can survive, because they are of same order of $k^2 \chi$. The following four terms in equation (3.41) are approximated under the Newtonian limit and re-expressed using the relations (3.22)-(3.23).

$$\begin{aligned} 6H \dot{H} z^2 \mathcal{A}_5 \chi &\approx -6\kappa \sigma z^2 \frac{\dot{H}}{H} \left(\frac{\nabla^2 \chi}{a^2} \right) \approx +6 \frac{\dot{H}}{H} \sigma z^2 \kappa Q_1, \\ 6H^2 z \dot{z} \mathcal{A}_5 \chi &\approx -6z \dot{z} \kappa \sigma \left(\frac{\nabla^2 \chi}{a^2} \right) \approx +6z \dot{z} \sigma \kappa Q_1, \\ 3H^2 z^2 \dot{\mathcal{A}}_5 \chi &\approx -3z^2 \kappa \left(\dot{\sigma} - \left(2H + 2 \frac{\dot{H}}{H} \right) \sigma \right) \left(\frac{\nabla^2 \chi}{a^2} \right) \approx +3z^2 \left(\dot{\sigma} - \left(2H + 2 \frac{\dot{H}}{H} \right) \sigma \right) \kappa Q_1, \\ 3H^2 z^2 \mathcal{A}_5 \dot{\chi} &\approx -3z^2 \kappa \sigma \left(\frac{\nabla^2 \dot{\chi}}{a^2} \right) \approx +3z^2 \sigma \kappa (\dot{Q}_1 + 2HQ_1). \end{aligned} \quad (3.42)$$

Those four approximated terms (3.42) are inserted into equation (3.41). By dividing by $3H^2 z^2$ and re-arranging the \dot{Q}_1 to one side, one can further simplify equation (3.41) due to some cancelling terms. The simplified form of equation (3.41) is then expressed in terms of N :

$$\begin{aligned} \frac{\kappa Q'_1}{3H^2 z^2} (1 - 3\sigma x^2 + 6\sigma z^2) &= \frac{\kappa Q_1}{3H^2 z^2} (3\sigma' x^2 + 6\sigma x \dot{x} - 6\sigma' z^2 - 12\sigma z \dot{z}) \\ &- 2 \left(\frac{H'}{H} + \frac{z'}{z} \right) \mathcal{A}_1 \delta_c - \mathcal{A}'_1 \delta_c - \mathcal{A}_1 \delta'_c. \end{aligned} \quad (3.43)$$

The conservation equation (2.16) is used to substitute z'/z and the normalised variables (3.25) are substituted into equation (3.43). The derivative \hat{q}_1 , which is required to complete equation (3.27), is thus obtained after some arrangement of equation (3.43):

$$\hat{q}_1 = \frac{3\tilde{Q}_1 (\sigma' x^2 + 2\sigma x x' - 2\sigma' z^2 - 4\sigma z z') + \left[(3 + \sqrt{3}\tilde{Q}_0 x) \delta_c - \delta'_c \right] \mathcal{A}_1 - \mathcal{A}'_1 \delta_c}{(1 - 3\sigma x^2 + 6\sigma z^2)}, \quad (3.44)$$

where,

$$\begin{aligned} \mathcal{A}'_1 = & -\frac{\lambda'_C}{2} - \sqrt{3} \left(\sigma' - \frac{H'}{H} \sigma \right) \left(x' - \frac{H'}{H} x \right) - \sqrt{3} \sigma \left(x'' + 2 \frac{H'}{H} x' + \frac{H''}{H} x \right) \\ & - \frac{3}{2} (\sigma' x^2 + 2\sigma x x') (\lambda_D - 2\lambda_C) - \frac{3\sigma x^2}{2} (\lambda'_D - 2\lambda'_C). \end{aligned} \quad (3.45)$$

4 Results

The disformally coupled quintessence model, which is described by the system of evolution equations (3.16) and (3.27), is solved numerically in order to obtain the perturbations δ_c and δ_b in terms of cosmological redshift $Z = 1/a - 1$. Note that the redshift Z is not to be confused with dynamical variable z .

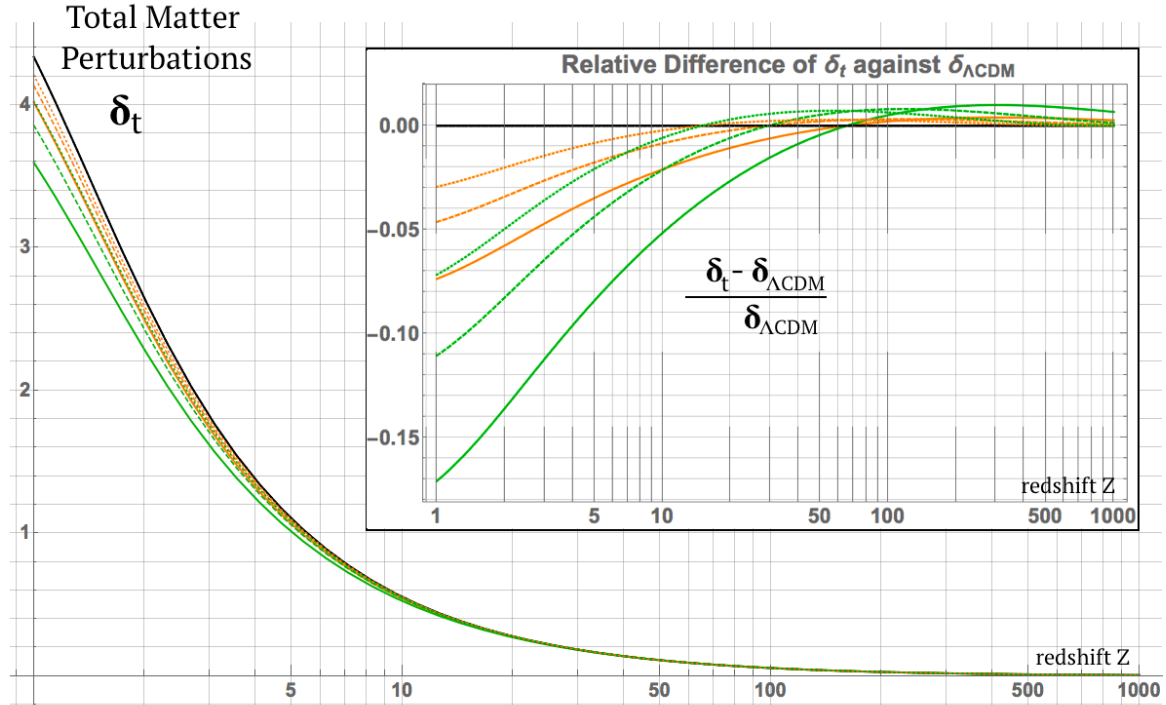


Figure 1. The effect of quintessential mass upon evolution of total matter perturbations. The black line represents Λ CDM while the orange lines and green solid lines correspond to $\alpha = 0.05$ and 0.08 respectively. For each color line, the solid, dashed, dotted lines correspond to $D_m = 0.001, 0.005, 0.01 \text{ meV}^{-1}$ respectively. $\sigma_8^0 = 0.818$ from [33] and β is set as unity.

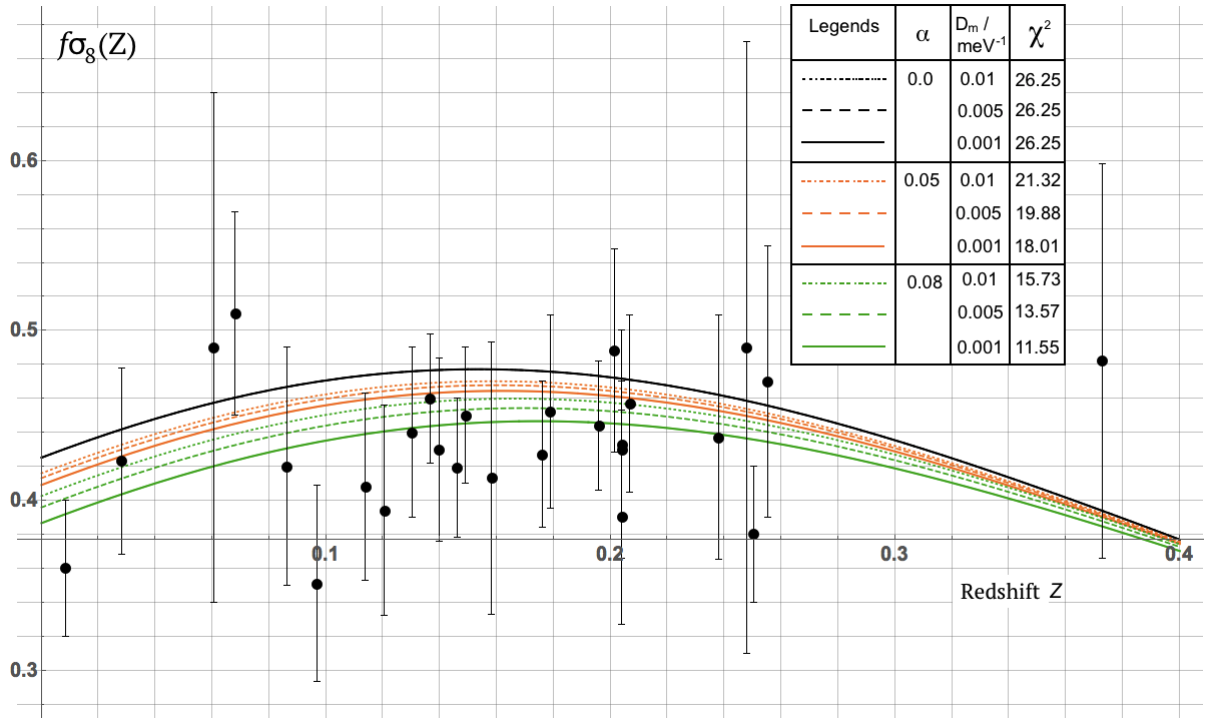


Figure 2. The effect of quintessential mass on the numerical $f\sigma_8(Z)$ curve of the disformally coupled quintessence model is shown with respect to redshift Z , together with RSD data [39–53]. The black line represents Λ CDM while the orange lines and green solid lines correspond to $\alpha = 0.05$ and 0.08 respectively. For each color line, the solid, dashed, dotted lines correspond to $D_m = 0.001, 0.005, 0.01 \text{ meV}^{-1}$ respectively. Other parameters are set as $\sigma_8^0 = 0.818$ from [33] and β as unity.

The perturbation equation (3.27) includes the normalised interaction term \tilde{Q}_0 in equation (2.18), the derivative \hat{q}_0 in equation (3.31), the normalised perturbed interaction term \tilde{Q}_1 in equation (3.39), and the derivative \hat{q}_1 in equation (3.44). Since the perturbation equations (3.16) and (3.27) also depend on background dynamical variables x and z , the numerical analysis requires solving the background dynamical system (2.15)–(2.18) simultaneously. From the above definition (2.14), one evaluates the initial values of the dynamical variables at redshift Z_i for an early universe according to the relations,

$$x_i = 0, \quad y_i = \sqrt{\frac{\Omega_{\Lambda 0}}{h_i^2}}, \quad z_i = \sqrt{\frac{\Omega_{\text{cdm}0}(1 + Z_i)^3}{h_i^2}}, \quad \sigma_i = \frac{D H_0^2}{\kappa^2 C} h_i^2, \quad h_i = h(Z_i), \quad (4.1)$$

where $h^2(Z) \equiv H^2/H_0^2$ is the reduced Hubble function and H_0 is Hubble parameter today. The density parameters $\Omega_{\text{cdm}0}$ and $\Omega_{\Lambda 0}$ correspond to DM and DE evaluated today. The initial values of redshift, density perturbations and their derivatives are set as:

$$Z_i = 10^4, \quad \text{and} \quad \delta_c(Z_i) = \delta_b(Z_i) = 10^{-3}, \quad \text{and} \quad \delta'_c = \delta'_b = 10^{-3}. \quad (4.2)$$

We shall now investigate how the density contrasts will eventually grow or decrease as the cosmological model enters into the non-linear regime for the given set of initial conditions (4.1) and (4.2). Observationally, the length scale $R_8 = 8h^{-1} \text{ Mpc}$ is defined as the spherical radius below which the linear regime is not valid. The parameter σ_8^0 is the present amplitude

of the matter power spectrum at the scale of R_8 [8]. Therefore, this disformally coupled quintessence model has four free parameters: σ_8^0 , α , β and D_m . For the analysis, we define (i) the total matter density perturbations δ_t , (ii) the growth function g , which describes the density perturbations with respect its current value, and (iii) the growth rate f , which indicates the rate of evolution for the total density perturbations [33]:

$$\delta_t \equiv \frac{\Omega_b \delta_b + z^2 \delta_c}{\Omega_b + z^2}, \quad g(Z) = \frac{\delta_t(Z)}{\delta_0} \quad \text{and} \quad f = \frac{d \ln \delta_t}{d \ln a} = \frac{\delta'_t}{\delta_t}, \quad (4.3)$$

such that $f\sigma_8(Z) = fg\sigma_8^0 = \left(\frac{\delta'_t}{\delta_0}\right) \sigma_8^0$,

where $f\sigma_8(Z)$ characterises the amount of clustering of galaxies at given redshift. Thus, after obtaining a numerical solution of δ_c and δ_b for a given choice of the parameters of the model, one can plot the numerical $f\sigma_8(Z)$ curve with respect to redshift Z . The disformal parameter β was found to have no appreciable effect on the evolution of total matter perturbation δ_t and $f\sigma_8(Z)$. The relative difference by percentage of δ_t as well as $f\sigma_8(Z)$ against the simplest disformal framework (with $\alpha = 0.08$, $\beta = 0.0$ and $D_m = 1.0$) is found to be $\leq 0.5\%$ and $\leq 0.35\%$ respectively, for any value of β in the range of $0 < \beta < 1000$. On the other hand, Figure 1 and Figure 2 show the effect of the quintessential mass on the evolution of the total matter perturbations δ_t , and the numerical $f\sigma_8(Z)$ curve respectively, whereby the parameters σ_8^0 and β values are set to be $\sigma_8^0 = 0.818$ and $\beta = 1.0$. The following remarks are made for both Figure 1 and Figure 2:

1. The Λ CDM model is recovered as expected when the conformal parameter α is set to zero, and is not affected by any choice of D_m .
2. For non-zero values of α and β , the conformal nature of the model dominates at lower values of D_m (i.e, higher mass M) and disformal framework becomes more significant at higher values of D_m (i.e lower mass M) as shown in [35].
3. Hence, with β set to unity and small D_m , the model behaves conformally, in that the conformal results as in [33] are recovered for $\alpha = 0.05$ and 0.08 .
4. For a fixed choice of α , the parameter D_m induces a gradual disformal effect. When D_m is very small (i.e, higher mass M), $f\sigma_8(Z)$ curve coincides with the purely conformal case, because the disformal coefficient $D(\phi)$ becomes zero, even if β is non-zero. As D_m is increased (i.e decreasing mass M), a disformal effect is induced such that the rate of evolution of δ_t then increases leading to higher $f\sigma_8(0)$ values. This means the structures cluster faster when compared to the respective conformal case.

Using Bayesian analysis, we investigated a multi-dimensional parameter space $\Theta_\mu \in \{\sigma_8^0, \alpha, \beta, D_m\}$ to find the best fit set of parameters. The main likelihood function is normalised to unity, $\int L(\Theta_\mu) d\Theta_\mu = 1$. It can also be marginalised over certain parameters i.e., by integrating these parameters out as, $L(\Theta_1) = \int L(\Theta_\mu) d\Theta_2 d\Theta_3 d\Theta_4$, to consider a sub-space of multi-dimensional parameter space [54]. Thus for example, $L(\Theta_1)$ is the Likelihood of Θ_1 only. In our analysis, the likelihood $L(\beta)$ is found to be equally probable for all values of β and therefore the parameter β is considered as degenerate. For this reason, the disformal parameter β is fixed to unity. The set of parameters is then reduced to $\Theta_\mu \in \{\sigma_8^0, \alpha, D_m\}$ only. A three-dimensional grid evaluation was carried out with $n = 75,000$ points to find the

most probable set of parameters, which most agree with the RSD data [39–53]. The bounds of the 3D parameters space are set as (i) $0.65 \leq \sigma_8^0 \leq 1.2$, (ii) $0 \leq \alpha \leq 0.5$, and (iii) $-5 \leq J \leq 0.0$, such that J is defined as $J = \log_{10} D_m$. The best fit set of parameters is found to be $\sigma_8^0 = 0.8 \pm 0.167$, $\alpha = 0.08 \pm 0.15$ and $D_m = 0.001 \pm 0.199$ within 68% confidence level (CL), at the minimum chi-square value $\chi^2_{\min} = 10.6931$. This implies that the observed RSD data favours an extremely low numerical value of D_m . In other words, as $D_m \rightarrow 0$, the quintessential mass $M \rightarrow \infty$ and therefore the observed RSD data prefers the model when it behaves conformally. The best fit set of parameters confirms the conformal constraints, previously obtained in [33]. The best fit value of the 3D grid for $\sigma_8^0 = 0.8 \pm 0.167$ within 68% CL seems to be agreement with Planck latest measured value of $\sigma_8 = 0.811 \pm 0.006$ [1].

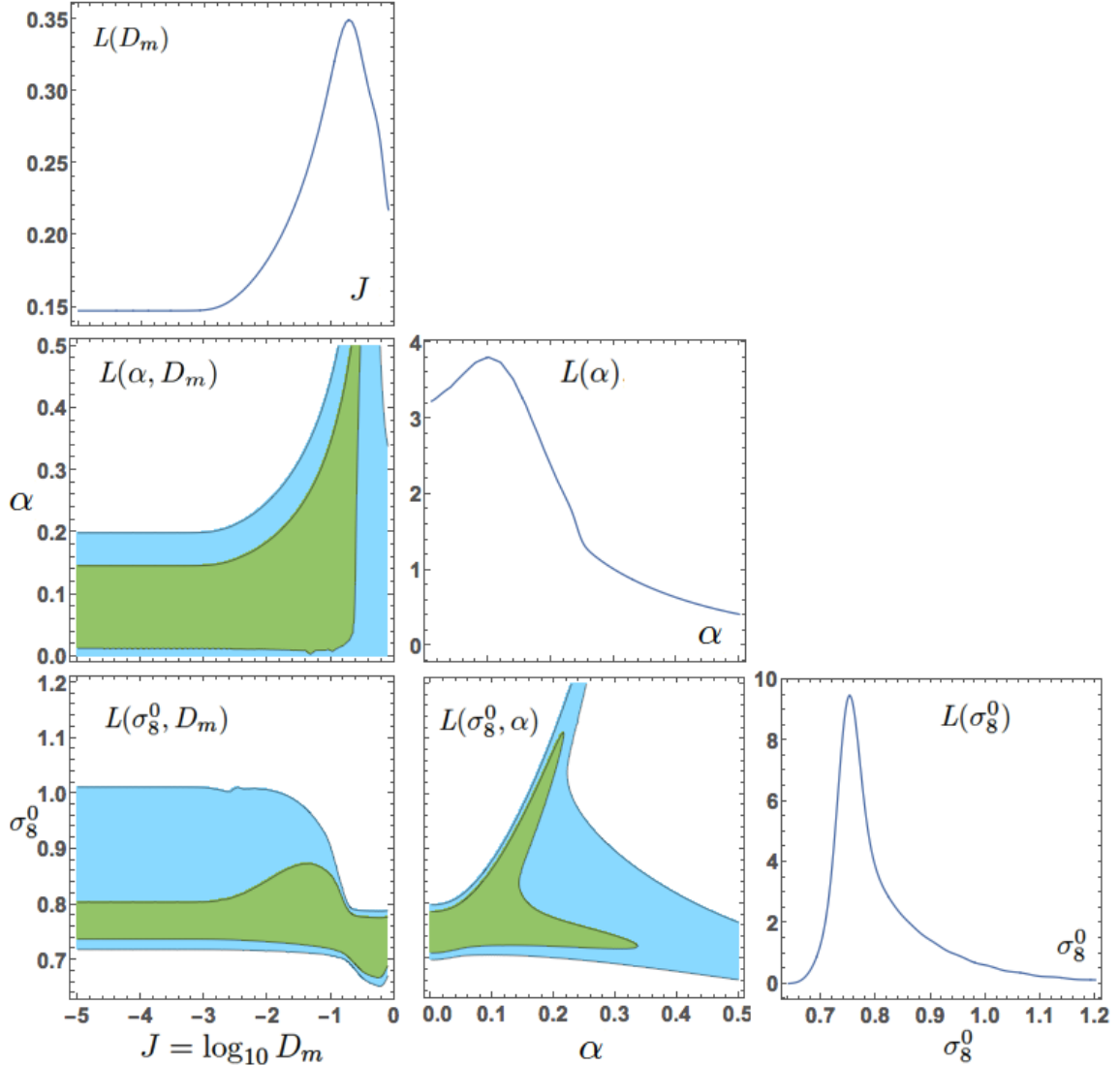


Figure 3. The marginalised surface Likelihoods $L(\alpha, D_m)$, $L(\sigma_8^0, D_m)$ and $L(\sigma_8^0, \alpha)$ are shown in the top view, where the green and the light blue regions indicate with 68% and 95% confidence as to where the correct set of parameters Θ_μ exists within each respective 2D parameters space. The marginalised likelihood curves $L(D_m)$, $L(\alpha)$, and $L(\sigma_8^0)$ are also shown.

Figure 3 shows the marginalisation of the main Likelihood $L(\Theta_\mu)$ over one parameter to yield the surface likelihoods $L(\alpha, D_m)$, $L(\sigma_8^0, D_m)$ and $L(\sigma_8^0, \alpha)$. These surface likelihoods are shown in the top view, where the green and the light blue regions indicate 68% and 95% confidence. Figure 3 also shows the marginalisation of the main Likelihood $L(\Theta_\mu)$ over two parameters to yield the 1D likelihood curves denoted by $L(D_m)$, $L(\alpha)$, and $L(\sigma_8^0)$. For range $0 < \alpha < 0.25$, the surface likelihood $L(\sigma_8^0, \alpha)$ maintains the characteristics of the conformal constraints with RSD data (See Figure 4 in [33]). The 1D likelihood curves $L(\alpha)$ and $L(\sigma_8^0)$ also manifest this reasoning. Any deviation from Figure 4 in [33] is attributed to the disformal dependence of this quintessence model. In the limit $D_m \rightarrow 0$, i.e., when the model starts to behave conformally, there can be various values of D_m for a given value of σ_8^0 in the surface Likelihood $L(\sigma_8^0, D_m)$. This appears similarly in the surface likelihood $L(\alpha, D_m)$ for a given value of α . This could suggest that the parameter D_m is actually degenerate in that limit. The Bayesian approach has shown that parameter β is degenerate and places some constraints on the three parameters σ_8^0 , α and D_m .

5 Conclusion

In this article and for the first time in the literature, we treated the perturbations of a disformally coupled quintessence model, whose background mimics the Λ CDM (See Section II). A derivation of the second order evolution equation for the density perturbations of the coupled fluid i.e, equation (3.27), was presented in Section 3.1. This derivation required the computation of the derivative of the disformal interaction term and its perturbation, which is shown in Subsection 3.2 and 3.3. The equation (3.27) reduces to the obtained perturbation equation in [33] in the conformal framework.

The disformally coupled quintessence model was analysed numerically by solving the system of evolution equations (3.27) and (3.16) to obtain δ_c and δ_b in terms of cosmological redshift. Using the definition (4.3), we plot the numerical $f\sigma_8(Z)$ curve for a chosen set of parameters. The effect of the quintessential mass is seen in the evolution of total matter perturbation (See Figure 1) and the numerical $f\sigma_8(Z)$ curve (See Figure 2). When a smaller quintessential mass is used for the model, a disformal effect seems to be induced. This disformal effect leads to faster rate of evolution for δ_t and higher $f\sigma_8(0)$ value, which implies that the large-scale structures cluster faster compared to the respective conformal case.

The free parameters of the model i.e. σ_8^0 , α , β , D_m were investigated with Bayesian statistics using the RSD data [39–53]. The parameter β was found to be degenerate because the likelihood $L(\beta)$ is a constant for all values of β . Figure 3 shows the marginalised surface likelihoods $L(\alpha, D_m)$, $L(\sigma_8^0, D_m)$ and $L(\sigma_8^0, \alpha)$ in topview, where the green and light blue indicate the 68% and 95% confidence regions. The best fit set of parameters is found to be $\sigma_8^0 = 0.8 \pm 0.167$, $\alpha = 0.08 \pm 0.15$ and $D_m = 0.001 \pm 0.199$ within 68% confidence level, at the minimum chi-square value $\chi_{\min} = 10.6931$. The best fit confirms the conformal results of the Ref. [33] and agrees with latest Planck value of $\sigma_8 = 0.811 \pm 0.006$ [1]. Thus, the model fits the RSD data very well when it behaves conformally.

6 Acknowledgements

AdLCD and AD acknowledge financial support from NRF Grants No.120390, Reference: BSFP190416431035, and No.120396, Reference: CSRP190405427545, and No 101775, Reference: SFH150727131568. AdLCD also acknowledges financial support from Project COOPB 204064, I-COOP+2019 CSIC Actions from the Spanish Ministry of Science, MICINN Project No. PID2019-108655GB-I00 from the European Regional Development Fund and Spanish Research Agency (AEI), and support from Projects Nos. CA15117 and CA16104 from COST Action EU Framework Programme Horizon 2020. AdLCD thanks the hospitality of the Institute of Theoretical Astrophysics - University of Oslo (Norway) during the later steps of the manuscript. AdLCD and NN also acknowledge funding from the University of Cape Town Visiting Scholars Fund 2018. This research was supported by Fundação para a Ciéncia e a Tecnologia (FCT) through the research grants: UIDB/04434/2020, UIDP/04434/2020, PTDC/FIS-OUT/29048/2017 (DarkRipple), COMPETE2020: POCI-01-0145-FEDER-028987 & FCT: PTDC/FIS-AST/28987/2017 (CosmoESPRESSO), CERN/ FIS-PAR/0037/2019 (MG-iCAP) and IF/00852/2015 (Dark Couplings). PKSD thanks First Rand Bank for financial support.

References

- [1] N. Aghanim *et al.* [Planck Collaboration], “Planck 2018 results. VI. Cosmological parameters,” arXiv:1807.06209 [astro-ph.CO].
- [2] H. Hildebrandt *et al.*, “KiDS-450: cosmological parameter constraints from tomographic weak gravitational lensing”, MNRAS, (2016), **465** no. 2, Pages 1454-1498, issn. 0035-8711, doi :10.1093/mnras/stw2805.
- [3] C. Heymans *et al.*, “CFHTLenS tomographic weak lensing cosmological parameter constraints: Mitigating the impact of intrinsic galaxy alignments”, MNRAS, (2013), **432**, No 3, Pages 2433-2453, issn: 0035-8711, doi: 10.1093/mnras/stt601.
- [4] V. Motta, M. A. García-Aspeitia, A. Hernández-Almada, J. Magaña and T. Verdugo, “Taxonomy of Dark Energy Models,” [arXiv:2104.04642 [astro-ph.CO]].
- [5] T. M. C. Abbott *et al.* [DES], “Dark Energy Survey year 1 results: Cosmological constraints from galaxy clustering and weak lensing,” Phys. Rev. D **98** (2018) no.4, 043526 doi:10.1103/PhysRevD.98.043526 [arXiv:1708.01530 [astro-ph.CO]].
- [6] A. Arbey and F. Mahmoudi, “Dark matter and the early Universe: a review,” doi:10.1016/j.ppnp.2021.103865 [arXiv:2104.11488 [hep-ph]].
- [7] Peacock, J. A. 1999, Cosmological Physics
- [8] P. Peter and J. P. Uzan, (Book): “Primordial Cosmology”, Published in: Oxford Graduate Texts, ISBN:9780199665150 (Print), 9780199209910 (eBook)
- [9] A. G. Riess *et al.* [Supernova Search Team], “Observational evidence from supernovae for an accelerating universe and a cosmological constant,” Astron. J. **116** (1998), 1009-1038 doi:10.1086/300499 [arXiv:astro-ph/9805201 [astro-ph]].
- [10] D. H. Weinberg, M. J. Mortonson, D. J. Eisenstein, C. Hirata, A. G. Riess and E. Rozo, “Observational Probes of Cosmic Acceleration,” Phys. Rept. **530** (2013), 87-255 doi:10.1016/j.physrep.2013.05.001 [arXiv:1201.2434 [astro-ph.CO]].
- [11] L. Verde, T. Treu and A. G. Riess, “Tensions between the Early and the Late Universe,” Nature Astron. **3**, 891 doi:10.1038/s41550-019-0902-0 [arXiv:1907.10625 [astro-ph.CO]].

- [12] S. Joudaki, H. Hildebrandt, D. Traykova, N. E. Chisari, C. Heymans, A. Kannawadi, K. Kuijken, A. H. Wright, M. Asgari and T. Erben, *et al.* *Astron. Astrophys.* **638** (2020), L1 doi:10.1051/0004-6361/201936154 [arXiv:1906.09262 [astro-ph.CO]].
- [13] A. G. Riess, L. M. Macri, S. L. Hoffmann, D. Scolnic, S. Casertano, A. V. Filippenko, B. E. Tucker, M. J. Reid, D. O. Jones and J. M. Silverman, *et al.* *Astrophys. J.* **826** (2016) no.1, 56 doi:10.3847/0004-637X/826/1/56 [arXiv:1604.01424 [astro-ph.CO]].
- [14] E. Di Valentino, O. Mena, S. Pan, L. Visinelli, W. Yang, A. Melchiorri, D. F. Mota, A. G. Riess and J. Silk, “In the Realm of the Hubble tension – a Review of Solutions,” [arXiv:2103.01183 [astro-ph.CO]].
- [15] D. Lovelock, “The Einstein tensor and its generalizations,” *J. Math. Phys.* **12** (1971), 498-501 doi:10.1063/1.1665613
- [16] D. Lovelock, “The four-dimensionality of space and the Einstein tensor,” *J. Math. Phys.* **13** (1972), 874-876 doi:10.1063/1.1666069
- [17] T. Clifton, P. G. Ferreira, A. Padilla and C. Skordis, “Modified Gravity and Cosmology,” *Phys. Rept.* **513** (2012) 1 doi:10.1016/j.physrep.2012.01.001 [arXiv:1106.2476 [astro-ph.CO]].
- [18] L. Amendola, “Coupled quintessence,” *Phys. Rev. D* **62** (2000), 043511 doi:10.1103/PhysRevD.62.043511 [arXiv:astro-ph/9908023 [astro-ph]].
- [19] D. J. Holden and D. Wands, “Selfsimilar cosmological solutions with a nonminimally coupled scalar field,” *Phys. Rev. D* **61** (2000), 043506 doi:10.1103/PhysRevD.61.043506 [arXiv:gr-qc/9908026 [gr-qc]].
- [20] B. Wang, E. Abdalla, F. Atrio-Barandela and D. Pavon, “Dark Matter and Dark Energy Interactions: Theoretical Challenges, Cosmological Implications and Observational Signatures,” *Rept. Prog. Phys.* **79** (2016) no.9, 096901 doi:10.1088/0034-4885/79/9/096901 [arXiv:1603.08299 [astro-ph.CO]].
- [21] F. F. Bernardi and R. G. Landim, “Coupled quintessence and the impossibility of an interaction: a dynamical analysis study,” *Eur. Phys. J. C* **77** (2017) no.5, 290 doi:10.1140/epjc/s10052-017-4858-x [arXiv:1607.03506 [gr-qc]].
- [22] J. D. Bekenstein, “The Relation between physical and gravitational geometry,” *Phys. Rev. D* **48** (1993) 3641 doi:10.1103/PhysRevD.48.3641 [gr-qc/9211017].
- [23] E. M. Teixeira, A. Nunes and N. J. Nunes, “Disformally Coupled Quintessence,” *Phys. Rev. D* **101** (2020) no.8, 083506 doi:10.1103/PhysRevD.101.083506 [arXiv:1912.13348 [gr-qc]].
- [24] R. Gannouji, M. W. Hossain, N. Jaman and M. Sami, “Bigravity and Horndeski gravity connected by a disformal coupling,” *Phys. Rev. D* **99** (2019) no.4, 043504 doi:10.1103/PhysRevD.99.043504 [arXiv:1808.04137 [gr-qc]].
- [25] P. Brax, A. C. Davis and A. Kuntz, “Disformally Coupled Scalar Fields and Inspiralling Trajectories,” *Phys. Rev. D* **99** (2019) no.12, 124034 doi:10.1103/PhysRevD.99.124034 [arXiv:1903.03842 [gr-qc]].
- [26] P. Brax, K. Kaneta, Y. Mambrini and M. Pierre, “Disformal dark matter,” *Phys. Rev. D* **103** (2021) no.1, 015028 doi:10.1103/PhysRevD.103.015028 [arXiv:2011.11647 [hep-ph]].
- [27] L. Xiao, R. An, L. Zhang, B. Yue, Y. Xu and B. Wang, “Can conformal and disformal couplings between dark sectors explain the EDGES 21-cm anomaly?,” *Phys. Rev. D* **99** (2019) no.2, 023528 doi:10.1103/PhysRevD.99.023528 [arXiv:1807.05541 [astro-ph.CO]].
- [28] D. Bettoni and S. Liberati, *Phys. Rev. D* **88** (2013), 084020 doi:10.1103/PhysRevD.88.084020 [arXiv:1306.6724 [gr-qc]].
- [29] M. Zumalacirregui and J. Garcia-Bellido, “Transforming gravity: from derivative couplings to

matter to second-order scalar-tensor theories beyond the Horndeski Lagrangian,” Phys. Rev. D **89** (2014) 064046 doi:10.1103/PhysRevD.89.064046 [arXiv:1308.4685 [gr-qc]].

[30] C. de Rham and G. Gabadadze, “Generalization of the Fierz-Pauli Action,” Phys. Rev. D **82** (2010) 044020 doi:10.1103/PhysRevD.82.044020 [arXiv:1007.0443 [hep-th]].

[31] T. Q. Do, “Higher dimensional nonlinear massive gravity,” Phys. Rev. D **93** (2016) no.10, 104003 doi:10.1103/PhysRevD.93.104003 [arXiv:1602.05672 [gr-qc]].

[32] T. Koivisto, D. Wills and I. Zavala, “Dark D-brane Cosmology,” JCAP **1406** (2014) 036 doi:10.1088/1475-7516/2014/06/036 [arXiv:1312.2597 [hep-th]].

[33] B. J. Barros, L. Amendola, T. Barreiro and N. J. Nunes, “Coupled quintessence with a Λ CDM background: removing the σ_8 tension,” JCAP **1901** (2019) 007 doi:10.1088/1475-7516/2019/01/007 [arXiv:1802.09216 [astro-ph.CO]].

[34] B. J. Barros, T. Barreiro and N. J. Nunes, Phys. Rev. D **101** (2020) no.2, 023502 doi:10.1103/PhysRevD.101.023502 [arXiv:1907.10083 [astro-ph.CO]].

[35] A. Dusoye, A. de la Cruz-Dombriz, P. Dunsby and N. J. Nunes, “Disformal couplings in a Λ CDM background cosmology,” JCAP **03** (2021), 002 doi:10.1088/1475-7516/2021/03/002 [arXiv:2006.16962 [gr-qc]].

[36] C. van de Bruck, J. Mifsud, J. P. Mimoso and N. J. Nunes, “Generalized dark energy interactions with multiple fluids,” JCAP **1611** (2016) 031 doi:10.1088/1475-7516/2016/11/031 [arXiv:1605.03834 [gr-qc]].

[37] C. van de Bruck and G. Sculthorpe, “Modified Gravity and the Radiation Dominated Epoch,” Phys. Rev. D **87** (2013) no.4, 044004 doi:10.1103/PhysRevD.87.044004 [arXiv:1210.2168 [astro-ph.CO]].

[38] C. P. Ma and E. Bertschinger, “Cosmological perturbation theory in the synchronous and conformal Newtonian gauges,” Astrophys. J. **455** (1995), 7-25 doi:10.1086/176550 [arXiv:astro-ph/9506072 [astro-ph]].

[39] S. de la Torre, L. Guzzo, J. A. Peacock, E. Branchini, A. Iovino, B. R. Granett, U. Abbas, C. Adami, S. Arnouts and J. Bel, *et al.* “The VIMOS Public Extragalactic Redshift Survey (VIPERS). Galaxy clustering and redshift-space distortions at $z=0.8$ in the first data release,” Astron. Astrophys. **557** (2013), A54 doi:10.1051/0004-6361/201321463 [arXiv:1303.2622 [astro-ph.CO]].

[40] H. Okada, T. Totani, M. Tonegawa, M. Akiyama, G. Dalton, K. Glazebrook, F. Iwamuro, K. Ohta, N. Takato and N. Tamura, *et al.* “The Subaru FMOS Galaxy Redshift Survey (FastSound). II. The Emission Line Catalog and Properties of Emission Line Galaxies,” Publ. Astron. Soc. Jap. **68** (2016) no.3, 47 doi:10.1093/pasj/psw043 [arXiv:1504.05592 [astro-ph.GA]].

[41] L. Guzzo, M. Pierleoni, B. Meneux, E. Branchini, O. L. Fevre, C. Marinoni, B. Garilli, J. Blaizot, G. De Lucia and A. Pollo, *et al.* Nature **451** (2008), 541-545 doi:10.1038/nature06555 [arXiv:0802.1944 [astro-ph]].

[42] C. H. Chuang, F. Prada, M. Pellejero-Ibanez, F. Beutler, A. J. Cuesta, D. J. Eisenstein, S. Escoffier, S. Ho, F. S. Kitaura and J. P. Kneib, *et al.* “The clustering of galaxies in the SDSS-III Baryon Oscillation Spectroscopic Survey: single-probe measurements from CMASS anisotropic galaxy clustering,” Mon. Not. Roy. Astron. Soc. **461** (2016) no.4, 3781-3793 doi:10.1093/mnras/stw1535 [arXiv:1312.4889 [astro-ph.CO]].

[43] C. Blake, “The WiggleZ Dark Energy Survey- joint measurements of the expansion and growth history at $z < 1$ ”, Mon. Not. Roy. Astron. Soc., **425** (2012) no. 1, pp. 405-414, doi:10.1111/j.1365-2966.2012.21473.x.

[44] M. Tegmark *et al.* [SDSS], “Cosmological Constraints from the SDSS Luminous Red Galaxies,”

Phys. Rev. D **74** (2006), 123507 doi:10.1103/PhysRevD.74.123507 [arXiv:astro-ph/0608632 [astro-ph]].

[45] H. Gil-Marín, W. J. Percival, J. R. Brownstein, C. H. Chuang, J. N. Grieb, S. Ho, F. S. Kitaura, C. Maraston, F. Prada and S. Rodríguez-Torres, *et al.* “The clustering of galaxies in the SDSS-III Baryon Oscillation Spectroscopic Survey: RSD measurement from the LOS-dependent power spectrum of DR12 BOSS galaxies,” Mon. Not. Roy. Astron. Soc. **460** (2016) no.4, 4188-4209 doi:10.1093/mnras/stw1096 [arXiv:1509.06386 [astro-ph.CO]].

[46] R. Tojeiro, “The clustering of galaxies in the SDSS-III Baryon Oscillation Spectroscopic Survey: measuring structure growth using passive galaxies”, Mon. Not. Roy. Astron. Soc., **424** (2012) no. 3, pp. 2339-2344 doi:10.1111/j.1365-2966.2012.21404.x.

[47] S. Satpathy *et al.* [BOSS], “The clustering of galaxies in the completed SDSS-III Baryon Oscillation Spectroscopic Survey: On the measurement of growth rate using galaxy correlation functions,” Mon. Not. Roy. Astron. Soc. **469** (2017) no.2, 1369-1382 doi:10.1093/mnras/stx883 [arXiv:1607.03148 [astro-ph.CO]].

[48] , L. Samushia, W. J. Percival, and A. Raccanelli, “Interpreting large-scale redshift-space distortion measurements”, Mon. Not. Roy. Astron. Soc. **420** (2012) no.3, pp. 2102-2119 doi:10.1111/j.1365-2966.2011.20169.x.

[49] C. Blake, “The WiggleZ Dark Energy Survey: the growth rate of cosmic structure since redshift $z=0.9$ ”, Mon. Not. Roy. Astron. Soc. , **415** (2011) no.3, pp. 2876-2891 doi:10.1111/j.1365-2966.2011.18903.x.

[50] W. J. Percival *et al.* [2dFGRS], “The 2dF Galaxy Redshift Survey: Spherical harmonics analysis of fluctuations in the final catalogue,” Mon. Not. Roy. Astron. Soc. **353** (2004), 1201 doi:10.1111/j.1365-2966.2004.08146.x [arXiv:astro-ph/0406513 [astro-ph]].

[51] C. Howlett, A. Ross, L. Samushia, W. Percival and M. Manera, “The clustering of the SDSS main galaxy sample – II. Mock galaxy catalogues and a measurement of the growth of structure from redshift space distortions at $z = 0.15$,” Mon. Not. Roy. Astron. Soc. **449** (2015) no.1, 848-866 doi:10.1093/mnras/stu2693 [arXiv:1409.3238 [astro-ph.CO]].

[52] F. Beutler, “The 6dF Galaxy Survey: $z \approx 0$ measurements of the growth rate and σ_8 ”, Mon. Not. Roy. Astron. Soc. **423** (2012) no.4, pp. 3430-3444 doi:10.1111/j.1365-2966.2012.21136.x.

[53] Y. S. Song and W. J. Percival, “Reconstructing the history of structure formation using Redshift Distortions,” JCAP **10** (2009), 004 doi:10.1088/1475-7516/2009/10/004 [arXiv:0807.0810 [astro-ph]].

[54] William H. Press and Saul A. Teukolsky, (1992) (Book): “Numerical Recipes in C : the Art of Scientific Computing”, Published in: Cambridge [Cambridgeshire] ; New York :Cambridge University Press, (ISBN 0-521-43108-5)